

Non-Stationarity Index in Vibration Fatigue: Theoretical and Experimental Research

Lorenzo Capponi^a, Martin Česnik^b, Janko Slavič^{b,1}, Filippo Cianetti^a, Miha Boltežar^b

^a *University of Perugia, Department of Engineering, via G. Duranti 93, 06125 Perugia, Italy*

^b *University of Ljubljana, Faculty of Mechanical Engineering, Aškerčeva 6, 1000 Ljubljana, Slovenia*

Cite as:

**Lorenzo Capponi, Martin Česnik, Janko Slavič, Filippo Cianetti and
Miha Boltežar,
Non-Stationarity Index in Vibration Fatigue: Theoretical and
Experimental Research,
International Journal of Fatigue, 2017,
DOI: 10.1016/j.ijfatigue.2017.07.020**

Abstract

Random vibrations induce damage in structures, especially when they are operating close to their natural frequencies. The stationarity of the input excitation is one of the fundamental assumptions required for frequency-domain fatigue-damage theory. However, for real applications, excitation is frequently non-stationary and the identification of this non-stationarity is not easy. This study researches run-tests to identify the index of non-stationarity. Further, using excitation signals with different rates of amplitude-modulated non-stationarity, the index of non-stationarity is experimentally and theoretically researched with regards to the fatigue life. The experimental research was performed on a flexible structure that was excited close to a natural frequency. The experimental fatigue life is compared to the theoretical fatigue life under the stationarity assumption. The analysis of the experimental results reveals a close relation

¹Corresponding author. Tel.: +386 14771 226. Email address: janko.slavic@fs.uni-lj.si

between the identified non-stationarity in the excitation signal and the fatigue life of the structure. It was found that amplitude-modulated non-stationary excitation results in a significantly shorter fatigue life if compared to a similar level of stationary excitation.

Keywords: Fatigue Damage, Vibration Fatigue, Non-Stationary signals, Non-Stationarity index, Experiment

1. Introduction

In vibration fatigue a random excitation interacts with a flexible structure. If during harmonic excitation the frequency is at, or close to, the structure's natural frequency, due to resonance, the fatigue increases significantly. Similarly, if broadband random excitation is applied, then the frequency content of the excitation couples with the structural dynamics of the structure; vibration fatigue deals with the high-cycle fatigue of flexible structures [1–3]. While the structural dynamics for most cases relies on the assumption of linearity [4], the stationarity of the input excitation is one of the fundamental assumptions required for frequency-domain fatigue-damage theory [5, 6]. However, for real applications, the excitation is frequently non-stationary (*e.g.*, a sudden load increase, changes in road roughness, turbulence loads) [7, 8]. The random processes are considered to be weakly stationary if the mean values as well as the covariance functions are time independent, and strongly (also strictly) stationary if the probability distributions are time independent [5]. If the definition is clear, the identification and the rate of non-stationarity are not. To identify the non-stationarity of an excitation, Rouillard [9] adopted the non-parametric “run-test” method of time-history signal evaluation to obtain the non-stationarity level of a vehicle's vibrations.

A structure's fatigue life under variable loading can be estimated using the rainflow-counting method [10], which is one of the most used time-domain methods and does not require the hypothesis of stationarity. On the other hand, the

frequency-counting methods [11, 12] are more powerful and require less computational effort when compared to the time methods, which makes them the first choice for addressing the fatigue damage of vibrating structures. In recent years a significant effort was invested into the further development of frequency methods from two aspects: the multi-axial stress state [13, 14], and non-Gaussianity and the non-stationarity of excitation signals [6, 15, 16]. Benasciutti *et al.* [17] studied the applicability of frequency-domain methods for the case of switching loads with partial Gaussian portions. Additional research on the signal decomposition in Gaussian portions was presented by Wolfsteiner [15] with direct applicability to frequency-counting methods. An alternative approach to dealing with non-Gaussian loads was introduced by Åberg *et al.*, [18] who established a new model for evaluating random loads, based on a Laplace-driven moving average.

When dealing with a vibration-fatigue phenomenon, a structure’s dynamic response appears as an additional intermediary between the dynamic load and the structure’s stress time history. According to Rizzi *et al.* [19], a stationary non-Gaussian random excitation of a dynamic structure results in a Gaussian random displacement and stress response. This observation was further investigated by Kihm *et al.* [20] by focusing on the changes in kurtosis when comparing the excitation and the response signals. The proposed kurtosis rate law was validated with numerical simulations of a linear dynamic system. In both studies [19, 20] the authors determined that for stationary loads the non-Gaussian excitation signal results in a Gaussian stress response, therefore justifying the use of frequency-counting methods. The reason for such “normalization” of the response signal was found within the central-limit theorem [5], which exposes the excitation signal’s non-stationarity as the origin of the non-Gaussian response. In light of this an experimental research was performed by Palmieri *et al.* [6], where a significant difference in the vibration fatigue life was observed for the case of excitation signals with an identical power spectral density (PSD), identical kurtosis and different rates of amplitude-modulated non-stationarity.

This manuscript proposes a slightly adopted Rouillard’s [9] run-test approach and relates it to the vibration fatigue life of the dynamic structure. In this way a definition of the non-stationarity index γ is introduced in the manuscript. The applicability of the proposed non-stationarity index γ will be tested on a larger number of experimental fatigue tests. Further, the relationship between the amplitude-modulated non-stationarity and the fatigue life will be researched.

This manuscript is organized as follows. In Section 2, the theoretical background is shown and methods to evaluate the rate of non-stationarity are introduced. In Section 3 the experimental research is defined: the experiment setup and the implementation of non-stationarity quantifying methods are presented in detail. In Section 4 the results of the fatigue tests are given and related to the previously calculated, non-stationarity index. Section 5 draws the conclusions.

2. Theoretical Background

This section gives the theoretical background to the dynamic response of structures, the damage accumulation in the time and frequency domains, the stationary processes and the identification of non-stationarity.

2.1. Structural Dynamics

The aim of the dynamic analysis of flexible structures is to evaluate the response of the structures excited by dynamic loads. A flexible structure can be represented by a multi-degree-of-freedom system (MDOF) [21] as:

$$\mathbf{M}\ddot{\mathbf{x}}(t) + \mathbf{D}\dot{\mathbf{x}}(t) + \mathbf{K}\mathbf{x}(t) = \mathbf{F}(t), \quad (1)$$

where \mathbf{M} , \mathbf{D} and \mathbf{K} are the mass, damping and stiffness matrices, respectively. \mathbf{F} is the excitation force and \mathbf{x} are the displacements of the degrees of freedom. In general, Eq. (1) represents a coupled system of differential equations. For the case of the proportional damping model the decoupling of equations is

possible via modal decomposition [21, 22], where the eigenvalue problem has to be solved. The resulting eigenfrequencies and eigenmodes characterize the dynamic properties of the structure. Using modal decomposition [23], Eq. (1) can be rewritten as:

$$\mathbf{I} \ddot{\mathbf{q}} + [\backslash 2 \xi \omega_0 \backslash] \dot{\mathbf{q}} + [\backslash \omega_0^2 \backslash] \mathbf{q} = \tilde{\Phi}^T \mathbf{f}, \quad (2)$$

where \mathbf{q} are the modal coordinates, \mathbf{I} is the identity matrix, $[\backslash 2 \xi \omega_0 \backslash]$ is related to the viscous damping and $[\backslash \omega_0^2 \backslash]$ is the diagonal matrix of the squared natural frequencies. The physical coordinates \mathbf{x} can be related to the modal coordinates \mathbf{q} :

$$\mathbf{x} = \Phi \mathbf{q}, \quad (3)$$

where Φ is the mass-normalized modal matrix, constructed from eigenvectors. Once the natural frequencies and the modeshapes are obtained, it is possible to write the frequency response function of the system, which is [24]:

$$H_{jk}(\omega) = \sum_{r=1}^n \frac{\phi_{jr} \phi_{kr}}{\omega_r^2 - \omega^2 + 2i\xi_r \omega_r \omega}, \quad (4)$$

where ϕ_{jr} and ϕ_{kr} are the elements of the matrix Φ , r iterates over the natural frequencies and modeshapes and the indexes j and k correspond to the response and excitation location, respectively [21].

In a similar way, the power spectral density of the excitation $\mathbf{S}_{x_0 x_0}$ can be related to the response stress tensor $\mathbf{S}_{\sigma\sigma}(\omega)$ via the FRF from the excitation x_0 to the stress response σ [16, 25]:

$$\mathbf{S}_{\sigma\sigma}(\omega) = \mathbf{H}_{\sigma x_0}^*(\omega) \cdot \mathbf{S}_{x_0 x_0}(\omega) \cdot \mathbf{H}_{\sigma x_0}^T(\omega), \quad (5)$$

where $\mathbf{H}_{\sigma x_0}^*(\omega)$ and $\mathbf{H}_{\sigma x_0}^T(\omega)$ are the complex conjugate and the transposed frequency response function matrix.

2.2. Damage Accumulation

Here time- and frequency-domain-based approaches will be used to determine the fatigue-damage accumulation [26]. Counting methods are typically

based on the application of Palmgren-Miner's rule [27]:

$$D = \sum_i \frac{n_i}{N_i}, \quad (6)$$

where D is the total fatigue damage, n_i is the number of cycles under a particular stress amplitude σ and N_i is the total number of cycles to failure associated with a particular stress amplitude σ . In theory, the fatigue failure occurs when the damage reaches 1. The relationship between the cycles and the properties of the material is described by Basquin's equation [28]:

$$\sigma = C N^{-\frac{1}{b}}, \quad (7)$$

where σ is the stress amplitude, C is the fatigue strength and b is the fatigue exponent, which describes the behavior of the Wöhler diagram [27].

In the time domain, the rainflow-counting method [10] reduces the stress time-history to a set of simple stress reversals [29]. In the frequency domain the fatigue damage is based on the spectral moments (which are obtained from the stress PSD) and on the properties of the materials. The i -th spectral moment m_i is defined as [5]:

$$m_i = \int_{-\infty}^{\infty} \omega^i S_{\sigma\sigma}(\omega) d\omega. \quad (8)$$

Bandwidth parameters can also describe the spectral density $S_{xx}(\omega)$, and the two most commonly used are:

$$\alpha_1 = \frac{m_1}{\sqrt{m_0 m_2}}, \quad \alpha_2 = \frac{m_2}{\sqrt{m_0 m_4}}. \quad (9)$$

Using the spectral moments of the signal and the material properties, the fatigue damage can be estimated, using different methods; a good overview was given in [11]. Here, the Tovo-Benasciutti method [26] will be used, as it was found to be more reliable than the Dirlik [30] approach [11].

2.3. Stationary Process

A random process $x_k(t)$ (k is the index of the process in an ensemble) is a stationary process whose joint probability distribution does not change over

time [5]. The random process $x_k(t)$ is weakly stationary if the mean value as well as the covariance function are time independent (equal for each t).

Further, a stochastic process is ergodic with respect to the mean and covariance function if the time average can be used instead of the ensemble average [31]:

$$\mu_x(k) = \lim_{T \rightarrow \infty} \frac{1}{T} \int_0^T x_k(t) dt, \quad (10)$$

$$C_{xx}(\tau, k) = \lim_{T \rightarrow \infty} \frac{1}{T} \int_0^T [x_k(t) - \mu_x(k)] [x_k(t + \tau) - \mu_x(k)] dt. \quad (11)$$

In other words, for weakly ergodic processes the time averages equal the ensemble averages, independently of the chosen k .

If a time series is stationary, then the classic theory allows us to evaluate the fatigue damage with both time- and frequency-domain approaches. However, the fatigue loadings acting on the mechanical components and structures could be random and as well as non-stationary [7] and therefore the frequency-domain approach is questionable.

In fact, vibration tests are usually conducted starting with measurements of the force or acceleration time history excitation applied to the structure. The time-domain measurement is used to obtain the power spectral density (PSD), which is further used for shaker testing. PSD is often used because it contains all the statistical information necessary to characterize the applied excitation, and allows us to estimate the expected load-cycle distribution, using simple analytical formulas [17]. However, this only holds if the stationary processes assumption is valid.

2.4. Index of Non-Stationarity

Quantifying the non-stationarity of a process can help us to know when a signal can be processed and analyzed with the classic theory of fatigue analysis as if it was stationary (even if it is not). In the literature [5, 32, 33], methods

to evaluate the non-stationarity of a process and to treat them are explained.

Run tests are used to identify non-stationarity. The run test is a non-parametric method based on the idea of dividing the signal to be analyzed in time-windows, and for every window calculate the variation of one of the statistical properties with respect to the same property of the entire signal [9]. It is based on the definition of a *run*, as a sequence of identical observations followed and preceded by a different observation or no observation at all [5]. It means that every window is assigned a value, for example (1) or (0), depending on the relationship between the statistical characteristics of the windowed signal and the conditions imposed by the test, and then the runs are evaluated. With the run-test approach, too few or too many of the runs can be the proof of non-stationarity [34]. Hence, the distribution of the number of the runs r in a sequence is a random variable r , which has a mean μ_r and variance σ_r^2 :

$$\mu_r = \frac{2N_1N_2}{N} + 1, \quad \sigma_r^2 = \frac{(2N_1N_2(2N_1N_2 - N))}{N^2(N - 1)}, \quad (12)$$

where N_1 and N_2 are the numbers of observations based on the conditions imposed by the test, and N is the total number of observations [9]. Once the level of significance is chosen, the confidence interval will be:

$$\mu_r \pm \alpha \sigma_r, \quad (13)$$

where α is the confidence coefficient: considering a level of 95% of confidence, α is equal to 1.96 [35]. Thus, if the number of runs falls inside the interval, the signal is supposed to be stationary, otherwise, it will be non-stationary. At the end, the number of runs is divided by the expected mean number of runs:

$$\gamma = \frac{r}{\mu_r} \quad [\%], \quad (14)$$

where γ is referred to as the non-stationarity index that indicates the level of non-stationarity of the process: numbers close to 1 should represent a stationary process.

Rouillard [9] defined the run-test $V(n)$ as:

$$V(n) = \begin{cases} 1; & R_w(n) > R_T \\ 0; & R_w(n) \leq R_T \end{cases}, \quad (15)$$

where R_w is the root-mean-square (RMS) value of the windowed signal, R_T is the average mean-square value for the entire sample record and n is the observation index of window.

In this research, the proposed assignation criterion is slightly different:

$$V(n) = \begin{cases} 1; & |R_w(n) - R_T| > \sigma_R \\ 0, & |R_w(n) - R_T| \leq \sigma_R \end{cases}, \quad (16)$$

where the RMSs of the window $R_w(n)$ and the average R_T are limited on both sides by the standard deviation of all the windows σ_R as:

$$\sigma_R = \sqrt{\frac{1}{N_w} \sum_{n=1}^{N_w} (R_w(n) - R_T)^2}, \quad (17)$$

where N_w is the total number of windows.

In contrast to Rouillard's one-sided approach the two-sided approach proposed here detects higher and lower values than the average of the entire sample record. The application of both methods on the time signal is presented in Fig. 1.

In previous research [9] it was shown that a run-test exhibits a high sensitivity to window width. A short window width can reveal rapid variations of the signal, which may not necessarily represent non-stationarities. On the other hand, if the window width is too wide, significant short-duration non-stationarities might not be detected.

3. Experimental Research

In this section the experimental research is presented. The signal generation and the experiment setup are explained, which are essential for the analysis of non-stationary signals and the evaluation of the obtained non-stationarity index γ .

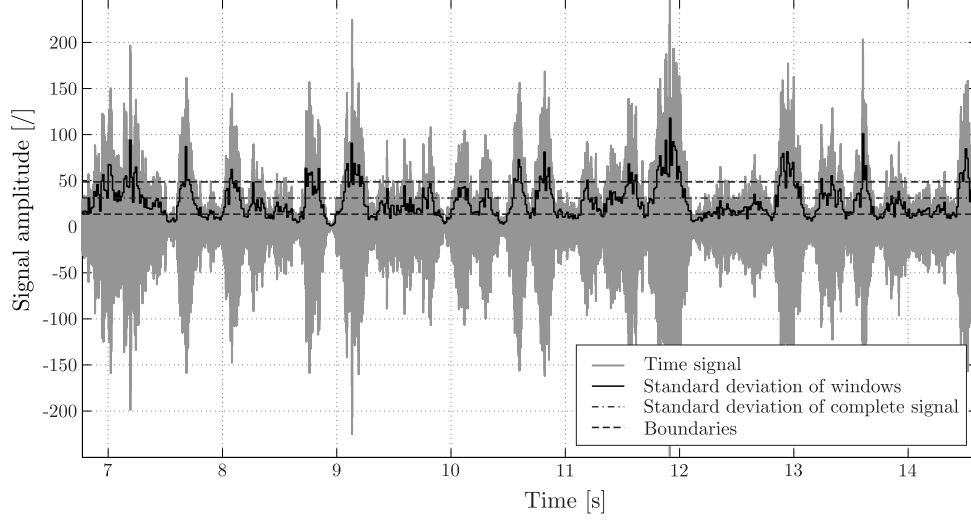


Figure 1: Run-test evaluation of a time signal.

3.1. Signal Generation

In order to investigate the influence of excitation non-stationarity on the actual fatigue life of a structure, a set of time signals with different non-stationarity rates was obtained first. For the bulk of physical phenomena the non-stationarity is exhibited as the time variance of a signal's power; the fluctuations in a signal's frequency content are less commonly observed. In the presented research a power time-variance was obtained with amplitude modulation *i.e.* by generating a stationary random signal with a known PSD and kurtosis and later multiplying it with a carrier-wave function [20]. The carrier wave is a low-frequency waveform that modulates the random stationary signal. In the presented research the carrier wave was generated using a beta distribution, since the relevance of this approach has been confirmed in studies by Palmieri *et al.* [6] and Kihm *et al.* [20]. In probability theory and statistics, the beta distribution is a family of continuous probability distributions defined for the interval $[0, 1]$, parametrized by two positive parameters, α and β , that control the shape of the distribution.

The probability density function (PDF) of the beta distribution is [36]:

$$p(x) = \frac{x^{\alpha-1}(1-x)^{\beta-1}(\Gamma(\alpha+\beta))}{\Gamma(\alpha)\Gamma(\beta)}, \quad (18)$$

where $\Gamma(z)$ represents the gamma function.

In order to concisely study how excitation's non-stationarity rate influences vibration fatigue life it is essential that PSD shape and kurtosis [5, 31, 37] remain invariable across all observed non-stationary signals. For this a special attention was given to the signal generation method for later experimental analysis:

1. A flat-shaped PSD function was defined in a frequency band from 600 Hz to 850 Hz, as shown in Fig. 2a). The frequency band was chosen to cover the 4th natural frequency of the tested specimen, see Fig. 3. Given the PSD a stationary Gaussian signal was generated, as shown in Fig. 2b).
2. A set of carrier waves was obtained by a cubic spline interpolation of the points produced by the beta distribution using different pairs of parameters α and β . The carrier wave that when multiplied by a stationary random signal resulted in a non-stationary signal with kurtosis 7 was chosen (not all the generated carrier waves corresponded to this criteria) as the primary carrier wave (Fig. 4a)) and was in the next step used for the signal generation. The time length of the primary carrier wave was 1800 seconds (30 minutes).
3. The next step was to prepare different signals with different rates of non-stationarity. This was done by squeezing the primary carrier wave 2, 4, 10, 50, 500 or 10,000 times. After squeezing, the new signal was repeated to reach the time length of 1800 seconds. In Fig. 5 the PSD of all 7 carrier waves is presented.
4. All the carrier waves were individually multiplied with a stationary Gaussian signal to obtain a set of random non-stationary signals; the kurtosis of all the random non-stationary signals was identified.

A total number of 8 different time signals was generated: squeezed 1, 2, 4, 10, 50, 500 and 10,000 times and stationary without the carrier wave. All the

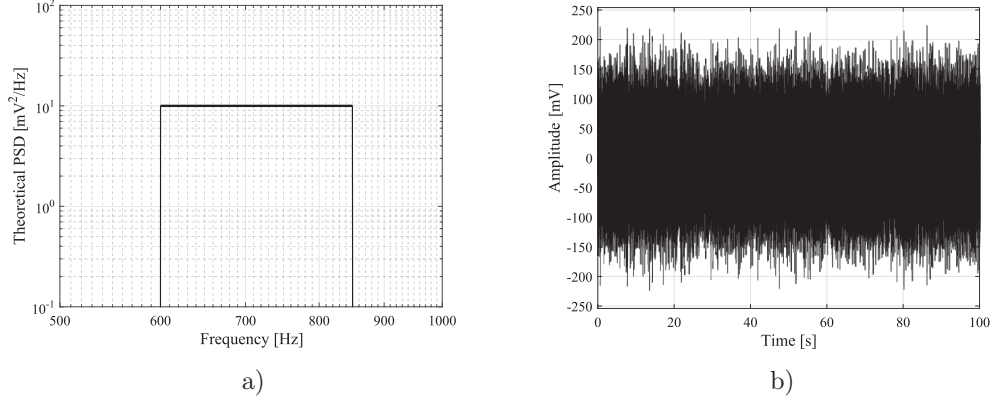


Figure 2: a) Flat PSD with amplitude level 10 mV^2/Hz and b) corresponding stationary time signal with root-mean-square value of 50 mV.

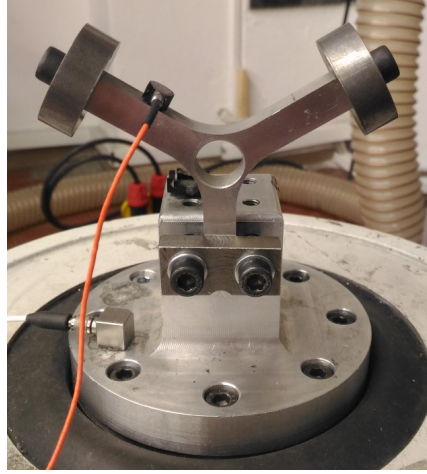


Figure 3: Y-shaped specimen with installed accelerometers.

time signals had the same PSD, the same time length, the same kurtosis, but different levels of non-stationarity. In this work the squeezed signals are denoted with SQ- i , where SQ stands for "squeezed" and i is the integer of how many times the carrier-wave is squeezed. The non-squeezed signal SQ-1 is presented in Fig. 4b). Squeezed signals SQ-10, SQ-50, SQ-500 and SQ-10000, that were

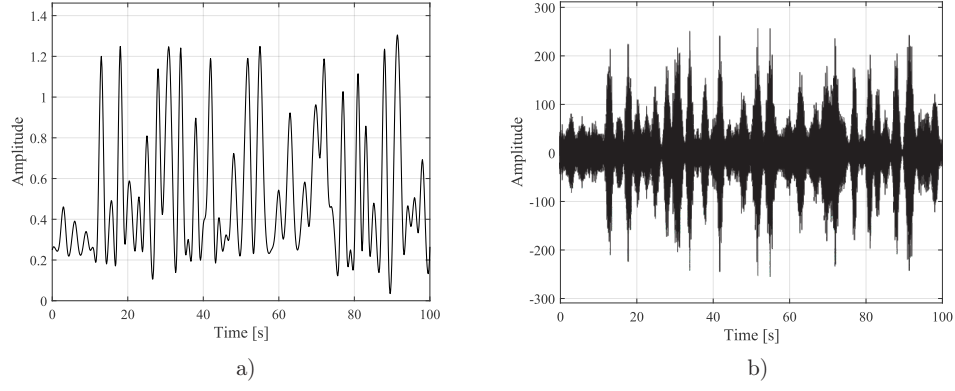


Figure 4: a) Primary carrier wave and b) and non-stationary time signal SQ-1.

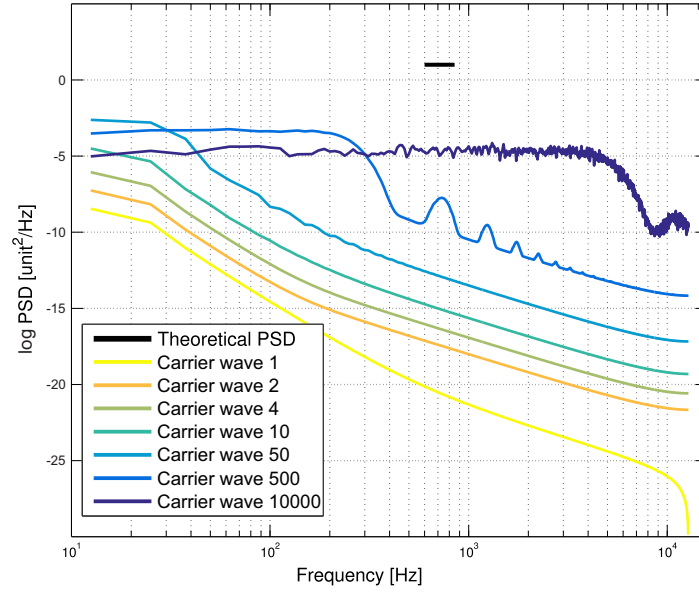


Figure 5: Power spectral density of the carrier waves.

later measured on electro-dynamic shaker (Sec. 3.2), are presented in Fig. 6.

3.2. Experiment Setup

In this research a Y-shaped specimen, shown in Fig. 3, was used [6, 38]. The specimen consists of three beams at 120° and with a cross-section of 10×10 mm.

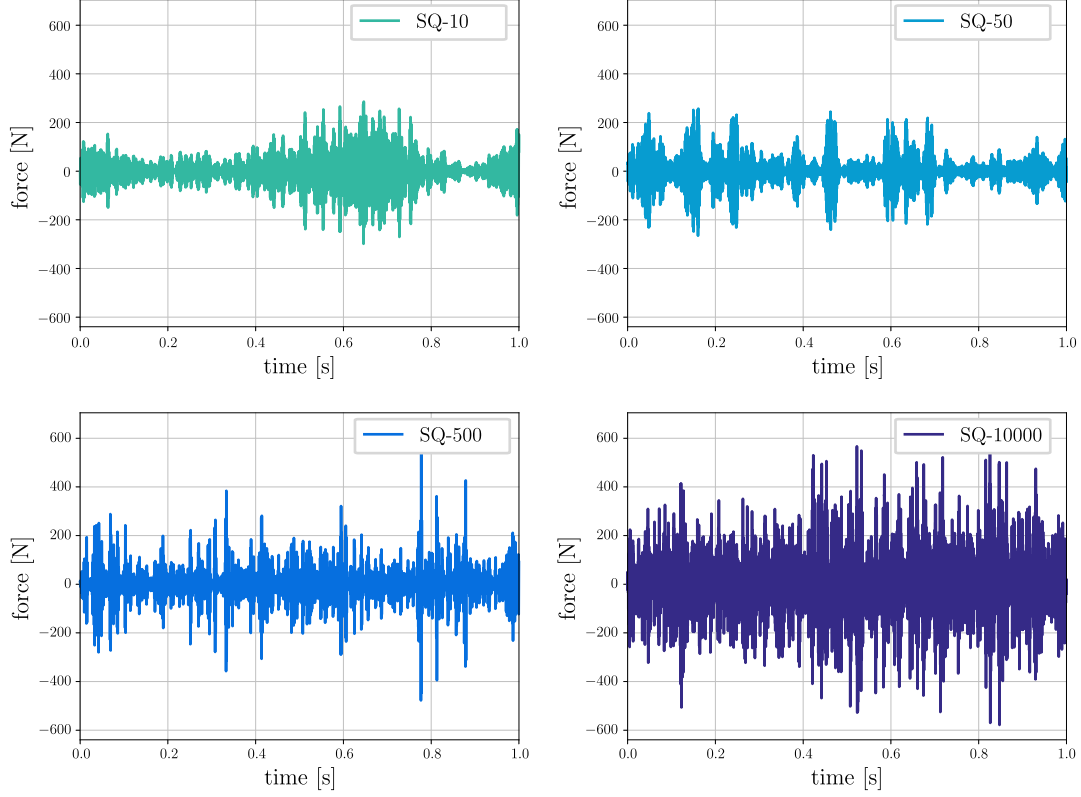


Figure 6: Time history of measured excitation signals SQ-10, SQ-50, SQ-500 and SQ-10000 with PSD level of $13.5 \text{ N}^2/\text{Hz}$.

The Y-specimen is made from cast aluminum alloy A-S8U3 with a density of 2710 kg/m^3 and a Young's modulus of $75,000 \text{ MPa}$. The specimen's surface was milled and the fatigue zone was additionally fine ground to remove imperfections that could lead to an untimely start of an initial crack. Weights with a mass of 52.5 g were fixed to each side, to adjust the natural frequencies of the Y-specimen: the fourth mode shape at $f_4 = \omega_4/(2\pi) \approx 775 \text{ Hz}$ was recognized as the most suitable for the near-resonance fatigue test [6]. For the experiment analysis the LDS V555 electro-dynamical shaker was used and the Y-specimen was attached to it with a fixation adapter. One accelerometer was installed on the specimen to measure its response; a second accelerometer was installed at

the base of the shaker to allow the control of the input signals, as shown in Fig. 3. The accelerometers were a Bruel&Kjær 4517-002 and a PCB T333B30, respectively, both connected to a NI-9234 24-bit ADC module. The driving voltage signal was generated with a NI-9263 16-bit DAC module. In both cases a sampling frequency of 25,600 Hz was used.

The experimental methodology for conducting the fatigue tests is presented next. First, the signal of the chosen squeezing was applied to the shaker with the fixation adapter, but without the Y-specimen. The input excitation signal was monitored and recorded with the accelerometer attached at the base of the shaker. By taking into account the mass of the shaker's armature and the fixation adapter, the PSD value of the excitation force was determined and manually set to the required level. After that, the Y-specimen was attached to the shaker and the fatigue test was performed with a known excitation force level. The measured excitation-force PSDs of signals SQ-1–SQ-10000 are presented in Fig. 7 together with response-acceleration of Y-specimen excited with signal SQ-10000.

During the test the Y-specimen's response was recorded in order to monitor the changes of the specimen's fourth natural frequency. This was later used to determine the time-to-failure of the specimen with a frequency-based damage-detection method [39]:

$$\omega_0^* = \omega_0 \cdot \sqrt{1 - Z}, \quad (19)$$

where ω_0^* denotes the natural frequency of the damaged specimen, ω_0 denotes the initial natural frequency of the undamaged specimen and Z is the fractional change in the frequency. In this research Z was chose to be 5% [38].

4. Results

The run test proposed in Eq. (16) was first used to obtain the non-stationarity index γ . Then the non-stationarity index γ was related to the vibration fatigue life.

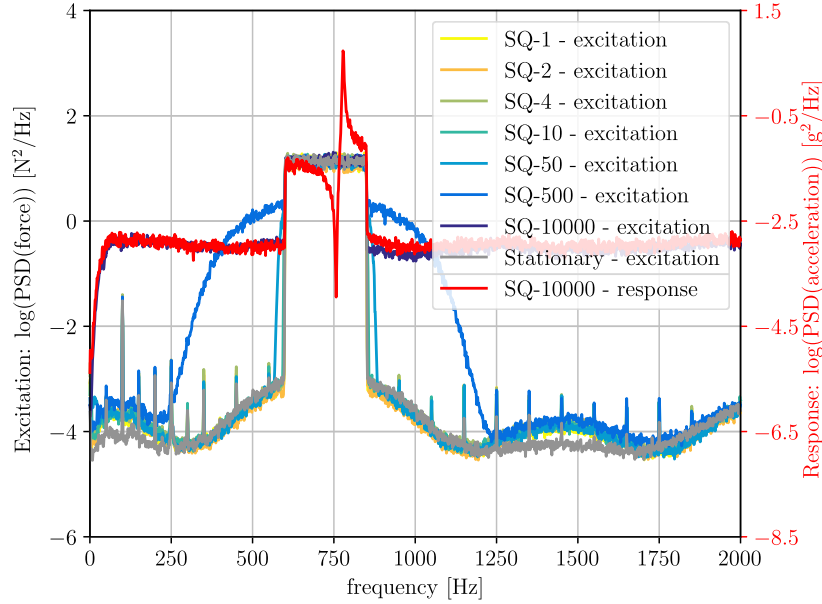


Figure 7: PSD spectrums of measured excitation-force signals with PSD level of $13.5 \text{ N}^2/\text{Hz}$ and Y-specimen's response-acceleration for excitation signal SQ-10000.

4.1. Non-stationarity index of measured excitation signals

As presented in Sec. 2.4 the window width Eq. (16) can have a significant effect on the identified non-stationarity index. For this purpose, *de facto* stationary signal and non-stationary signals SQ-1 - SQ-10000 were measured on the shaker's armature with a force PSD level of $13.5 \text{ N}^2/\text{Hz}$ (later more PSD levels will be added).

In total seven time-window widths were applied to the run-test, ranging from 0.005 to 1 second. In Tab. 1 the resulting non-stationarity indexes γ are given. Moreover, the influence of the window's width is graphically presented in Fig. 8. According to Rizzi *et al.* [19] the optimal window width is expected to be related to the period of the system's impulse response, *i.e.*, the time in which the response amplitude reduces to 10 % of the initial value [20]; in the case of the Y-specimen the period of the impulse response was experimentally determined to be in the range up to 0.2 seconds. By inspecting Fig. 8 a significant difference

between low squeezing and high squeezing is observed; at a window width of 0.04 s the signals SQ-1 to SQ-4 were identified as non-stationary, while the SQ-500, SQ-10000 and also the *de facto* stationary signal were identified as stationary. Similar results were found for other RMS values of the excitation signal.

Table 1: Non-stationarity index γ for two-sided method: results in bold identify signal as stationary. Set of excitation force with PSD level 13.5 N²/Hz.

Signal type	Window width						
	0.005 s	0.01 s	0.0125 s	0.02 s	0.04 s	0.1 s	1 s
Stationary	96 %	99 %	100 %	101 %	102 %	99 %	72 %
SQ-10000	96 %	101 %	101 %	101 %	102 %	100 %	101 %
SQ-500	95 %	97 %	99 %	99 %	102 %	105 %	90 %
SQ-50	73 %	86 %	92 %	98 %	95 %	96 %	114 %
SQ-10	65 %	62 %	61 %	61 %	72 %	96 %	109 %
SQ-4	64 %	60 %	57 %	50 %	46 %	67 %	105 %
SQ-2	65 %	60 %	58 %	50 %	40 %	39 %	104 %
SQ-1	66 %	62 %	60 %	53 %	40 %	31 %	96 %

4.2. Vibration fatigue testing

Here, the *de facto* stationary and squeezed signals SQ-1 - SQ-10000 were applied to the Y-specimen. According to a preliminary analysis of the excitation signals the non-stationarity index γ shows that the signals SQ-500, SQ-10000 can be considered as stationary and the signals SQ-1, SQ-2 and SQ-4 can be considered as non-stationary. This finding will now be tested against the vibration fatigue life.

For the sake of experimental comprehensiveness the time signals were applied to the Y-specimen at four different force PSD levels, as shown in Fig. 9. For each of the 19 combination pairs of excitation PSD level and signal type, two samples were tested for the fatigue life. In total, 41 samples were broken. Certain load

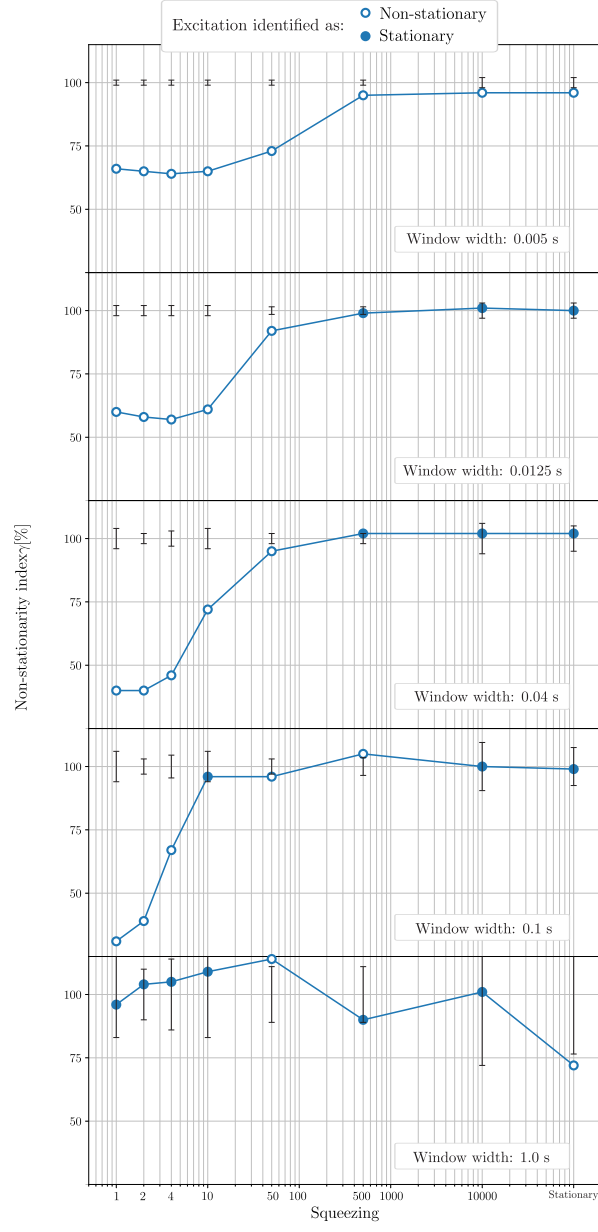


Figure 8: Window width's influence on the non-stationarity index γ of measured excitation signal for two-sided run-test method with denoted confidence intervals.

level and signal type combinations were left untested either due to instantaneous failure or due to the absence of failure after $2 \cdot 10^7$ load cycles. In Fig. 10 the relative natural frequency drop ω_0^*/ω_0 of 7 specimens excited with the same force PSD level of $13.5 \text{ N}^2/\text{Hz}$ is presented. By observing the natural frequency changes, a significant influence of the signal type on the fatigue life can be observed.

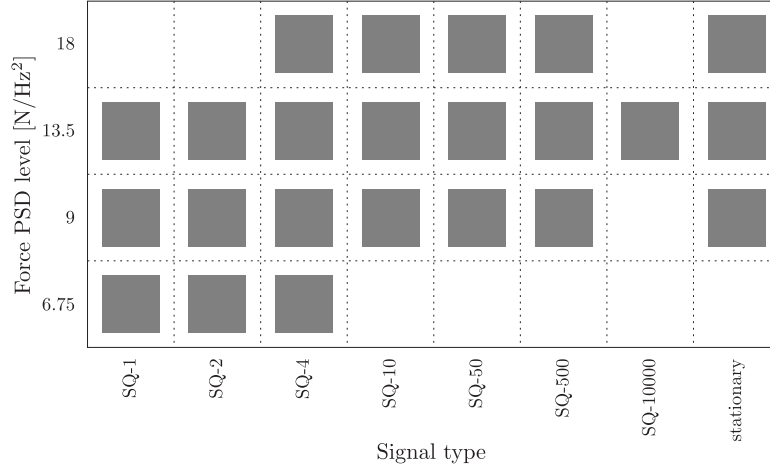


Figure 9: Experimentally tested combinations of signal types and excitation levels.

The fatigue life for all the tested specimens is given in Tab. 2. It is clear that squeezing the carrier wave and thus changing the non-stationarity rate significantly changes the fatigue life, see Fig. 11. From Fig. 11 it is clear that for the SQ-4 the fatigue life is significantly shorter than for the *de facto* stationary signal, while SQ-50 is in between.

Due to the considerable influence of the non-stationarity rate on the fatigue life only tests with an excitation force PSD level of $13.5 \text{ N}^2/\text{Hz}$ were possible on the complete set of generated non-stationary signals SQ-1 - SQ-10000 and on the *de facto* stationary signal, see Tab. 2. To better understand Fig. 11, a detailed analysis of the PSD level of $13.5 \text{ N}^2/\text{Hz}$ is shown in Fig. 12: one axis shows the fatigue life, the other axis shows the non-stationarity index. It was previously shown that the excitation from SQ-1 to SQ-4 can be considered as

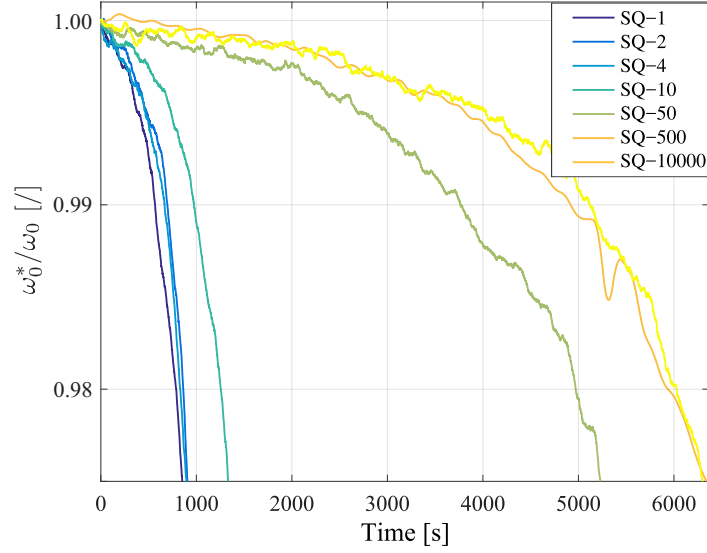


Figure 10: Relative change of the fourth natural frequency during excitation with non-stationary signals having force PSD level of $13.5 \text{ N}^2/\text{Hz}$.

Table 2: Experimental fatigue lives [s] of tested Y-specimens.

Force PSD level [N^2/Hz]	Signal type							
	SQ-1	SQ-2	SQ-4	SQ-10	SQ-50	SQ-500	SQ-10000	Stationary
18	/	/	643	598	999	1624	/	3157
			341	497	1069	2793		
13.5	961	871	737	1175	1120	4069	6299	4428
	857	907	899	1333	5234	6411	6309	
9	2364	2853	3279	3177	3722	>12600	/	>12600
	2994	2391	2899	3824	5894			
6.75	5112	2737	4429	/	/	/	/	/
	4865	4405	5435					

non-stationary, while the SQ-500 and above can be considered as stationary. As all the time signals had the same PSD, the same time length, the same kurtosis, but the signals differ in the levels of non-stationarity resulting in significant

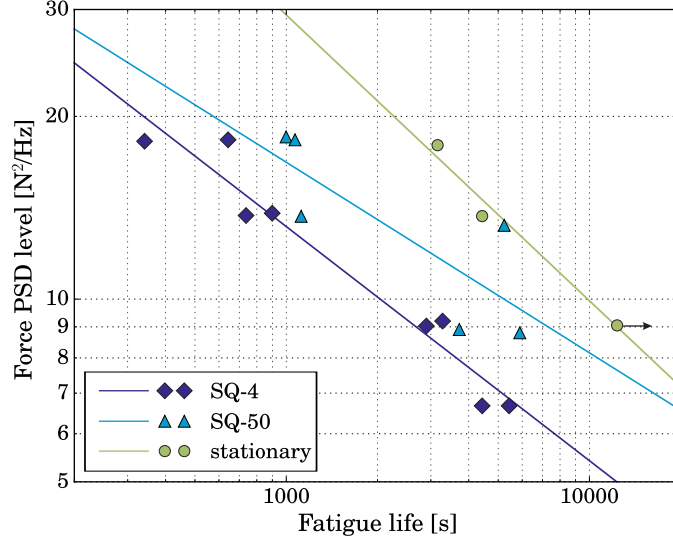


Figure 11: Experimental fatigue life for the representative excitation signal types: SQ-4, SQ-50 and *de facto* stationary.

differences in fatigue life. The difference between non-stationary and stationary conditions is approximately 5 fold.

Fig. 13 shows the normed fatigue life (the normalization is to the fatigue life during stationary excitation). From the results of all 41 tested samples it is clear that the excitation identified as non-stationary resulted in a reduced fatigue life to approximately 20%. Signals that are not clearly stationary, nor are they non-stationary, have a fatigue life between the two groups.

5. Conclusions

This study researches the influence of amplitude-modulated non-stationary excitation on the experimental fatigue life of flexible structures. Excitation is frequently non-stationary in terms of time-varying power and the question is what rate of non-stationarity can still be considered as stationary and how does the rate of non-stationarity effect the fatigue life?

To research the non-stationarity, experimental tests were performed using

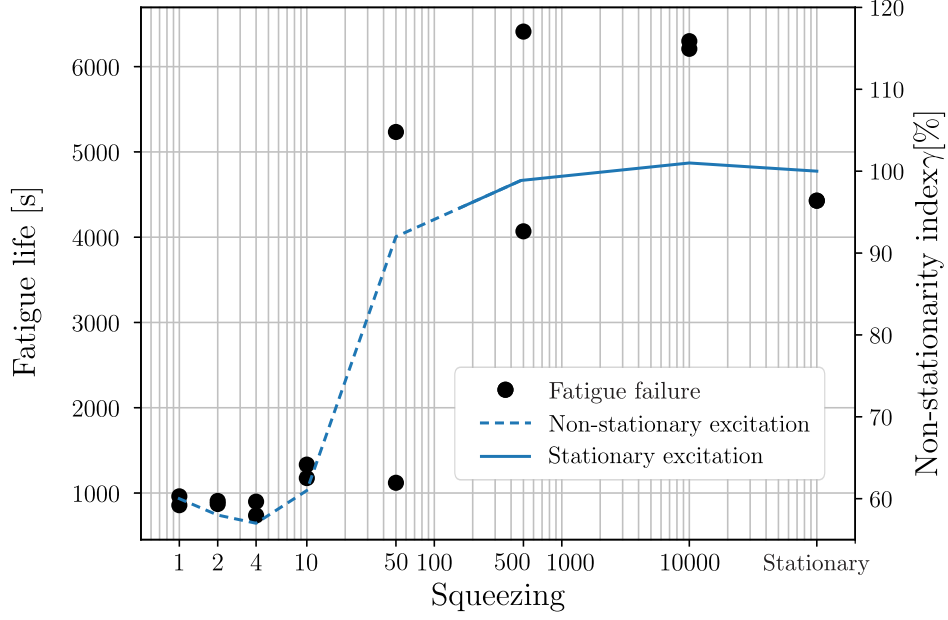


Figure 12: Comparison of experimental fatigue lives for excitation PSD level of $13.5 \text{ N}^2/\text{Hz}$ and excitation signal's non-stationarity index γ for window width of 0.0125 using two-sided run-test method.

squeezed signals with the same PSD and kurtosis, but different rates of non-stationarity. The study was applied to a Y-shaped specimen. Several tests were performed and repeated, considering four different levels of the power spectral density. An enhanced method to identify the non-stationarity was proposed and resulted in a clear differentiation of the non-stationarity in the signal.

The signals that were identified as non-stationary resulted in a significantly shorter fatigue life of the sample than the ones that were identified (or were *de facto*) stationary.

Finally, the non-stationarity identification relates on the natural frequencies of the researched structure. However, if the non-stationarity is identified during the excitation, the resulting fatigue life was shown to significantly decrease (in this research to 1/5th).

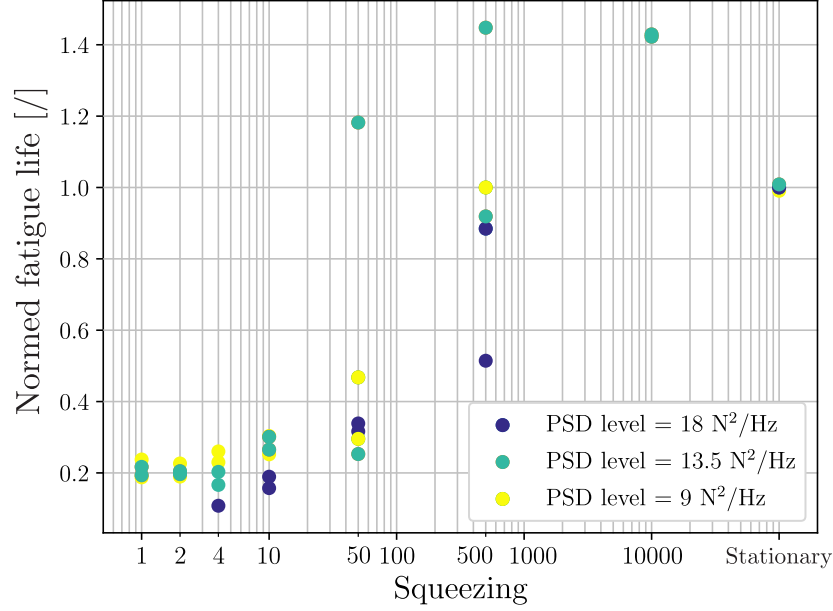


Figure 13: Fatigue lives of Y-specimens, normed to fatigue life under *de facto* stationary excitation signal.

Acknowledgment

The authors acknowledge the partial financial support from the Slovenian Research Agency (research core funding No. P2-0263 and J2-6763).

- [1] D. Benasciutti, F. Sherratt, A. Cristofori, Recent developments in frequency domain multi-axial fatigue analysis, *International Journal of Fatigue* 91 (2016) 397–413.
- [2] M. Mršnik, J. Slavič, M. Boltežar, Vibration fatigue using modal decomposition, *Mechanical Systems and Signal Processing* (2017) in press.
- [3] A. Niesłony, M. Böhm, Frequency-domain fatigue life estimation with mean stress correction, *International Journal of Fatigue* 91 (2016) 373–381.
- [4] A. K. Chopra, *Dynamics of Structures: Theory and Applications to Earthquake Engineering*, 3rd Edition, Prentice Hall, New Jersey, 1995.

- [5] J. S. Bendat, A. G. Piersol, Random Data: Analysis and Measurement Procedures, 4th Edition, John Wiley & Sons, Inc., New Jersey, 2010.
- [6] M. Palmieri, M. Česnik, J. Slavič, F. Cianetti, M. Boltežar, Non-Gaussianity and non-stationarity in vibration fatigue, *International Journal of Fatigue* 97 (2017) 9–19.
- [7] G. P. Nason, R. Von Sachs, G. Kroisandt, Wavelet processes and adaptive estimation of the evolutionary wavelet spectrum, *Journal of the Royal Statistical Society: Series B (Statistical Methodology)* 62 (2) (2000) 271–292.
- [8] W. Zhang, C. S. Cai, F. Pan, Y. Zhang, Fatigue life estimation of existing bridges under vehicle and non-stationary hurricane wind, *Journal of Wind Engineering and Industrial Aerodynamics* 133 (2014) 135–145.
- [9] V. Rouillard, Quantifying the Non-stationarity of Vehicle Vibrations with the Run Test, *Packaging Technology and Science* 27 (3) (2014) 203–219.
- [10] M. Matsuishi, T. Endo, Fatigue of metals subjected to varying stress, *Japan Society of Mechanical Engineers, Fukuoka, Japan* 68 (2) (1968) 37–40.
- [11] M. Mršnik, J. Slavič, M. Boltežar, Frequency-domain methods for a vibration-fatigue-life estimation – Application to real data, *International Journal of Fatigue* 47 (2013) 8–17.
- [12] C. Braccesi, F. Cianetti, G. Lori, D. Pioli, Random multiaxial fatigue: A comparative analysis among selected frequency and time domain fatigue evaluation methods, *International Journal of Fatigue* 74 (2015) 107–118.
- [13] D. Benasciutti, F. Sherratt, A. Cristofori, Basic Principles of Spectral Multi-axial Fatigue Analysis, *Procedia Engineering* 101 (2015) 34–42.
- [14] W. Xu, X. Yang, B. Zhong, G. Guo, L. Liu, C. Tao, Multiaxial fatigue investigation of titanium alloy annular discs by a vibration-based fatigue test, *International Journal of Fatigue* 95 (2017) 29–37.

- [15] P. Wolfsteiner, Fatigue assessment of non-stationary random vibrations by using decomposition in Gaussian portions, *International Journal of Mechanical Sciences* (2016) in press.
- [16] C. Braccesi, F. Cianetti, L. Tomassini, Fast evaluation of stress state spectral moments, *International Journal of Mechanical Sciences* (2016) in press.
- [17] D. Benasciutti, R. Tovo, Frequency-based fatigue analysis of non-stationary switching random loads, *Fatigue & Fracture of Engineering Materials & Structures* 30 (11) (2007) 1016–1029.
- [18] S. Åberg, K. Podgórski, I. Rychlik, Fatigue damage assessment for a spectral model of non-Gaussian random loads, *Probabilistic Engineering Mechanics* 24 (4) (2009) 608–617.
- [19] S. A. Rizzi, A. Przekop, T. L. Turner, On the Response of a Nonlinear Structure to High Kurtosis Non-Gaussian Random Loadings, in: *Proceedings of the 8th International Conference on Structural Dynamics, EURO-DYN 2011*, Leuven, Belgium, 2011.
- [20] F. Kihm, S. A. Rizzi, N. S. Ferguson, A. Halfpenny, Understanding how kurtosis is transferred from input acceleration to stress response and it's influence on fatigue life, in: *Proceedings of the XI International Conference on Recent Advances in Structural Dynamics*, Pisa, Italy, 2013.
- [21] N. M. M. Maia, J. M. M. Silva, *Theoretical and Experimental Modal Analysis*, 1st Edition, Research Studies Press Ltd., Baldock, Hertfordshire, 1997.
- [22] C. Braccesi, F. Cianetti, A procedure for the virtual evaluation of the stress state of mechanical systems and components for the automotive industry: Development and experimental validation, *Proceedings of the Institution of Mechanical Engineers, Part D: Journal of Automobile Engineering* 219 (5) (2005) 633–643.

- [23] M. G  radin, D. J. Rixen, Mechanical Vibrations: Theory and Application to Structural Dynamics, 3rd Edition, John Wiley & Sons, Ltd, Chichester, West Sussex, 2015.
- [24] D. J. Ewins, Modal Testing: Theory, Practice and Application, 2nd Edition, Research Studies Press, Ltd., Baldock, Hertfordshire, 2000.
- [25] M. Haiba, D. C. Barton, P. C. Brooks, M. C. Levesley, Review of life assessment techniques applied to dynamically loaded automotive components, Computers & Structures 80 (5-6) (2002) 481–494.
- [26] D. Benasciutti, Fatigue analysis of random loadings, Ph.D. thesis, University of Ferrara, Italy (2004).
- [27] R. C. Juvinall, K. M. Marshek, Fundamentals of Machine Component Design, 3rd Edition, John Wiley & Sons, Inc., New York, 2003.
- [28] O. H. Basquin, The exponential law of endurance tests, Proceedings of American Society of Testing Materials 10 (1910) 625–630.
- [29] C. Amzallag, J. P. Gerey, J. L. Robert, J. Bahuaud, Standardization of the rainflow counting method for fatigue analysis, International Journal of Fatigue 16 (4) (1994) 287–293.
- [30] T. Dirlik, Application of computers in fatigue analysis, Ph.D. thesis, University of Warwick, UK (1985).
- [31] K. Shin, J. K. Hammond, Fundamentals of Signal Processing for Sound and Vibration Engineers, 1st Edition, John Wiley & Sons, Ltd, Chichester, West Sussex, 2008.
- [32] H. B. Nielsen, Non-Stationary Time Series and Unit Root Testing (2007).
- [33] C. Hory, N. Martin, A. Chehikian, Spectrogram Segmentation by Means of Statistical Features for Non-Stationary Signal Interpretation, IEEE Transactions on Signal Processing 50 (12) (2002) 2915–2925.

- [34] M. R. Masliah, Stationarity/nonstationarity identification, Tech. rep., University of Toronto, Canada (2004).
- [35] H. M. Walker, J. Lev, Statistical inference, 1st Edition, Holt, Rinehart & Winston, New York, 1953.
- [36] V. K. Rohatgi, A. K. M. E. Saleh, An Introduction to Probability and Statistics, 3rd Edition, John Wiley & Sons, Inc., New Jersey, 2015.
- [37] D. E. Newland, Random vibrations, spectral and wavelet analysis, 3rd Edition, Longman, Essex, 1993.
- [38] M. Mršnik, J. Slavič, M. Boltežar, Multiaxial vibration fatigue-A theoretical and experimental comparison, Mechanical Systems and Signal Processing 76 (2016) 409–423.
- [39] J.-T. Kim, Y.-S. Ryu, H.-M. Cho, N. Stubbs, Damage identification in beam-type structures: frequency-based method vs mode-shape-based method, Engineering Structures 25 (1) (2003) 57–67.

List of Figures

1	Run-test evaluation of a time signal.	10
2	a) Flat PSD with amplitude level $10 \text{ mV}^2/\text{Hz}$ and b) corresponding stationary time signal with root-mean-square value of 50 mV	12
3	Y-shaped Specimen	12
4	a) Primary carrier wave and b) and non-stationary time signal SQ-1.	13
5	Power spectral density of the carrier waves.	13
6	Time history of measured excitation signals SQ-10, SQ-50, SQ-500 and SQ-10000 with PSD level of $13.5 \text{ N}^2/\text{Hz}$	14
7	PSD spectrums of measured excitation-force signals with PSD level of $13.5 \text{ N}^2/\text{Hz}$ and Y-specimen's response-acceleration for excitation signal SQ-10000.	16
8	Window width's influence on the non-stationarity index γ of measured excitation signal for two-sided run-test method with denoted confidence intervals.	18
9	Experimentally tested combinations of signal types and excitation levels.	19
10	Relative change of the fourth natural frequency during excitation with non-stationary signals having force PSD level of $13.5 \text{ N}^2/\text{Hz}$	20
11	Experimental fatigue life for the representative excitation signal types: SQ-4, SQ-50 and <i>de facto</i> stationary.	21
12	Comparison of experimental fatigue lives for excitation PSD level of $13.5 \text{ N}^2/\text{Hz}$ and excitation signal's non-stationarity index γ for window width of 0.0125 using two-sided run-test method.	22
13	Fatigue lives of Y-specimens, normed to fatigue life under <i>de facto</i> stationary excitation signal.	23

List of Tables

1	Non-stationarity index γ for two-sided method: results in bold identify signal as stationary. Set of excitation force with PSD level $13.5 \text{ N}^2/\text{Hz}$	17
2	Experimental fatigue lives [s] of tested Y-specimens.	20